

On the low-field Hall coefficient of graphite

P. Esquinazi,* J. Krüger, and J. Barzola-Quiquia

*Division of Superconductivity and Magnetism, Institut für Experimentelle Physik II,
Universität Leipzig, Linnéstraße 5, D-04103 Leipzig, Germany*

R. Schönemann, T. Herrmannsdörfer

Hochfeld-Magnetlabor, Helmholtz-Zentrum Dresden-Rossendorf, Germany

N. García

*Laboratorio de Física de Sistemas Pequeños y Nanotecnología,
Consejo Superior de Investigaciones Científicas, E-28006 Madrid, Spain*

We have measured the temperature and magnetic field dependence of the Hall coefficient (R_H) in three, several micrometer long multigraphene samples of thickness between ~ 9 to ~ 30 nm in the temperature range 0.1 to 200 K and up to 0.2 T field. The temperature dependence of the longitudinal resistance of two of the samples indicates the contribution from embedded interfaces running parallel to the graphene layers. At low enough temperatures and fields R_H is positive in all samples, showing a crossover to negative values at high enough fields and/or temperatures in samples with interfaces contribution. The overall results are compatible with the reported superconducting behavior of embedded interfaces in the graphite structure and indicate that the negative low magnetic field Hall coefficient is not intrinsic of the ideal graphite structure.

I. INTRODUCTION

The Hall effect is a fundamental transport property of metals and semiconductors. It can provide information on the carrier densities as well as on other interesting features of the electronic band structure. Surprisingly and in spite of considerable work in the past, the Hall coefficient (R_H) of graphite, a highly anisotropic material composed by a stack of graphene layers with Bernal stacking order (ABA...), in particular the temperature and magnetic field dependence of R_H reported in literature is far from clear. For example, early data on the low-field Hall coefficient obtained in single-crystalline natural graphite (SCNG) samples showed that it is *positive* at fields below and negative above ~ 0.5 T at a temperature $T = 77$ K¹, suggesting that holes are the majority carriers. This result appears to be at odd to several other studies on the graphite band structure obtained in highly oriented pyrolytic graphite (HOPG) samples²⁻¹⁰ that suggest that electrons are the majority carriers, unless one argues in terms of different mobilities of the majority carriers, an interpretation that was used indeed in the past.

The difference between the reported Hall coefficient obtained in the SCNG and different HOPG samples was the subject of a short paper in 1970 where the authors concluded that the positive low-field Hall coefficient is observed for samples with long enough mean free path, i.e. less lattice defects, whereas the negative sign results from boundary scattering in HOPG samples due to the relatively small single crystalline grains¹¹. At high enough applied magnetic fields or high enough temperatures, this coefficient, however, turned negative^{1,11}. A positive low-field Hall coefficient was already reported in 1953 for graphite samples with small crystal size (less annealing temperature); it decreased with temperature

and changed sign at a sample dependent temperature¹². When the crystalline grain size in the samples was larger than ~ 0.5 μm , the Hall coefficient was always negative, at least at $T \geq 77$ K¹². Similar results were obtained in carbons and polycrystalline graphite samples with different crystal size in Ref. 13, where the authors recognized further that the Hall coefficient was highly dependent on the *alignment* of crystallites in the samples. Note that these two last reports^{12,13} are in apparent contradiction to the relationship between crystal size and positive sign of R_H given in Ref. 11. It is therefore suggestive that one extra parameter related to the alignment of the crystalline grains in the samples could provide a hint to solve this contradiction.

In the studies of Ref 14 a positive Hall coefficient was reported at 4.2 K that became negative at $\mu_0 H \geq 0.05$ T for different graphite samples. In that work¹⁴ the positive low-field Hall coefficient was explained within the two-band model arguing that it is due to the higher mobility of the majority holes in comparison with the mobility of the majority electrons. However, to understand its behavior as a function of field and temperature, three types of carriers had to be introduced in the calculations¹⁴. The low-field coefficient of different Kish graphite samples was reported in Ref. 15. For the “best” Kish sample, defined as the one with the largest resistivity ratio $\rho(300)/\rho(4.2)$, the Hall coefficient was positive at low fields and turned to negative at $\mu_0 H \simeq 0.6$ T at 4.2 K, similarly to the results for some of the graphite samples reported in Ref. 14. The temperature dependence of the zero-field Hall coefficient for the “best” Kish specimen was interpreted¹⁵ taking into account the trigonally warped Fermi surfaces in the standard Slonczewski-Weiss-McClure’s model^{16,17}. Interestingly, the lesser the perfection of the Kish graphite samples the larger was the field where the Hall coefficient changed sign¹⁵.

Ref.	year	sample	T – range	field – range	R_H	comment
12	1953	PCG	≥ 4.2 K	< 1 T	positive	for small grains only ³
13	1956	PCG	77 K/300 K	0.65 T	positive	for small grains only ⁴
1	1958	SCNG	≤ 77 K	< 0.5 T	positive	negative at large fields and temperatures
11	1970	HOPG/SCG	77 K	< 0.1 T	positive	negative upon mean free path ²
14	1974	(†)	4.2 K	< 50 mT	positive	negative at higher fields
15	1982	Kish graphite	4.2 K	< 600 mT	positive	$R_H(H)$ changes sign ⁵
20	2003	HOPG	$0.1 \text{ K} \leq T \leq 20 \text{ K}$	≤ 9 T	negative	quantum Hall effect (QHE) ⁶
18	2005	graphite flakes ¹	0.1 K	< 8 T	positive	
21	2006	HOPG	2 K, 5 K	≤ 9 T	negative	quantum Hall effect (QHE) ⁶
22	2006	HOPG	$0.1 \text{ K} \leq T \leq 100 \text{ K}$	≤ 0.5 T	negative	Anomalous Hall effect
8	2010	NG/HOPG	10 mK	< 10 T	negative	(*)
19	2011	graphite flakes ¹	$77 \leq T \leq 300 \text{ K}$	< 1 T	positive	

TABLE I. Selected publications that report on the Hall coefficient R_H of different graphite samples at different fields and temperatures. NG: natural graphite, SCNG: single crystal natural graphite, PCG: polycrystalline graphite. ¹Peeled off from HOPG. ² $R_H > 0$ for long mean free path, $R_H < 0$ for short mean free path or at higher fields. ³Negative for grain size $> 0.5\mu\text{m}$. Crossover from positive to negative at a sample dependent temperature. ⁴Positive R_H^0 for small grains, negative for grain size $> 0.5\mu\text{m}$, and strong orientation dependence of R_H^0 . ⁵ Turns negative at large field for samples with imperfect structure. ⁶With electrons as majority carriers. (*): No Hall data shown at low fields. (†): The samples were obtained by crystallization from a solution of carbon in iron and then purified at 2000°C in a flux of chlorine. The platelets had a thickness of $\sim 100 \mu\text{m} \lesssim d \lesssim 9 \text{ mm}$.

Recently published Hall measurements in micrometer small and thin graphite flakes, peeled off from HOPG samples, showed a positive and nearly field independent Hall coefficient at $T = 0.1$ K up to 8 T applied fields¹⁸. A positive Hall coefficient was also observed in similar graphite flakes at $77 \leq T \leq 300$ K, which decreased with temperature, it was field independent to $\mu_0 H \simeq 1$ T, decreasing at higher fields¹⁹. Interestingly, both results^{18,19} are in rather good quantitative agreement with the result for the low-field Hall coefficient reported 56 years ago for the bulk SCNG¹, in clear contrast to reports in HOPG bulk samples^{2,8,11,20–22}.

Further studies on bulk HOPG samples showed the existence of an anomalous Hall effect and a negative Hall coefficient at low fields, interpreted as the result of a mag-

netic field induced magnetic excitonic state²². Also the quantum Hall effect (QHE) (with electrons as majority carriers) has been reported in some bulk HOPG samples at high enough fields^{20,21}. But the QHE in graphite as well as other interesting features of the Hall effect behavior like the hole-like contribution with zero mass²³ in bulk HOPG samples, appear to be strongly sample dependent⁸. A short resume of the literature results can be seen in Table I. Evidently, all these, apparently contradictory results indicate us that we need a re-evaluation of the sign, temperature and field behavior of the Hall coefficient. The whole reported studies show us that we do not know with certainty, which is the *intrinsic* value of the Hall coefficient in ideal graphite and which is the origin of all the observed differences between samples of different origins and microstructure.

In this work, we argue that one main reason for the observed differences of the Hall coefficient between samples is related to the existence of two dimensional (2D) interfaces^{24–26}. Moreover, in some of them Josephson

coupled superconducting regions exist, oriented parallel to the graphene layers of the graphite matrix^{27–29}. The interfaces in graphite, whose contribution to the Hall effect we discuss in this work, are grain boundaries between

crystalline domains with slightly different orientations. Those crystalline domains and the two-dimensional borders between them, can be recognized by transmission electron microscopy when the electron beam is applied parallel to the graphene planes of graphite, see e.g. Fig. 1 in Ref. 29, Fig. 1 in Ref. 25 or Figs. 2.2 and 2.9 in Ref. 24. The interfaces can be located at the borders of slightly twisted crystalline Bernal stacking order regions (ABA...) or between regions with Bernal and rhombohedral stacking order (ABCAB...) regions. They can be recognized usually by a certain gray colour in the TEM pictures^{25,29}. From TEM pictures we obtain that the distance between those interfaces can be between ~ 30 nm and several hundreds of nm upon sample^{25,28}. Therefore, the thinner the graphite sample the lower the probability to have interfaces and to measure their contribution to any transport property.

The twist angle θ_{twist} , i.e., a rotation with respect to the c -axis between single crystalline domains of Bernal graphite, may vary from $\sim 1^\circ$ to $< 60^\circ$ ³⁰ while the tilting angle of the grains with respect to the c -axis $\theta_c \lesssim 0.4^\circ$ for the best oriented pyrolytic graphite samples. As emphasized in Ref. 29, in case the twist angle is small enough, the grain boundary can be represented by a system of screw dislocations or a system of edge dislocations if the misfit is in the c -direction with an angle $\theta_c \neq 0$. A system of dislocations at the two-dimensional interfaces or topological line defects can have a large influence in the dispersion relation of the carriers^{31,32} and trigger localized high-temperature superconductivity³³.

There have been several theoretical studies predicting high temperature superconductivity at the rhombohedral (ABC) graphite surface³⁴⁻³⁶ or at interfaces between rhombohedral and Bernal (ABA) graphite^{37,38}. We note that rhombohedral graphite regions were also recognized embedded in bulk HOPG samples^{39,40}. Theoretical studies indicate an unusual dependence of the superconductivity at the surface of rhombohedral graphite or at the interfaces between rhombohedral and Bernal (ABA) graphite in multilayer graphene on doping³⁷. Furthermore, calculations indicate that high-temperature surface superconductivity survives throughout the bulk due to the proximity effect between ABC/ABA interfaces where the order parameter is enhanced³⁷. Following experimental results that indicate the existence of granular superconductivity at certain interfaces in bulk HOPG samples of high grade^{27,28,41}, it is then appealing to take the contribution of the interfaces in the behavior of the Hall effect into account. Doing this we are able to interpret several results from literature as well as the Hall coefficient obtained from three, micrometer small graphite flakes described below. The characteristics of the embedded interfaces, as for example their size or area⁴¹ or the twist angle between the two Bernal graphite blocks²⁹ can have a direct influence on the temperature and magnetic field dependence of the Hall coefficient of a graphite sample with interfaces. Furthermore, the alignment dependence reported earlier¹³ can be understood arguing that

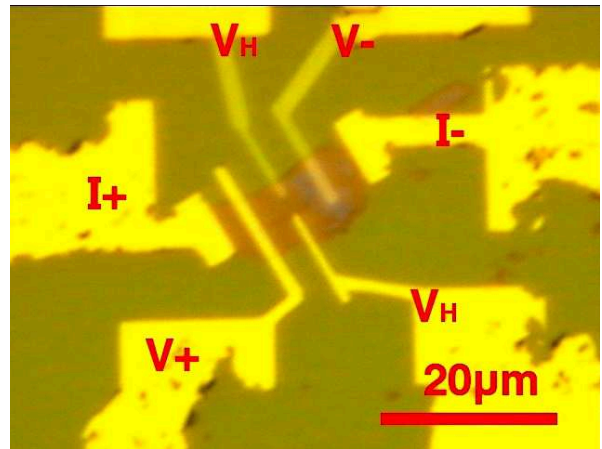


FIG. 1. Optical microscope picture of sample S1 with the two current and four voltage gold contacts after lithography development and evaporation of Pt/Au contacts.

the interfaces are created or get larger in area the higher the alignment of the grains. From the presented work we can conclude that the intrinsic low magnetic field Hall coefficient of ideal graphite is positive, i.e. hole like. It can change to negative in samples with embedded interfaces at fields and temperatures high enough to influence their contribution. On the other hand one expects that if the interfaces are not superconducting in a given sample, they will provide an electron-like contribution to the Hall resistance, which may or may not overwhelm the intrinsic Hall signal of graphite.

II. EXPERIMENTAL DETAILS

The graphite flakes we have measured were obtained by a rubbing method on Si-SiN substrates using a bulk HOPG sample of ZYA grade from Advanced Ceramics Co. These samples show, in general, well defined quasi-two dimensional interfaces between Bernal graphite structures with slightly different orientation around the c -axis. Their distance in the c -axis direction is sample dependent and in general < 500 nm and of several micrometer length in the (a, b) plane^{24,25,28}. The Pt/Au contacts for longitudinal and transverse Hall resistance measurements were prepared using electron beam lithography. The samples with their substrates were fixed on a chip carrier. Further details on the preparation can be read in²⁵. We have measured three samples labeled S1, S2 and S3 with similar lateral dimensions but with thickness: 9 ± 1 nm (S2), 20 ± 4 nm (S1) and 30 ± 3 nm (S3). An example of one of the samples is shown in Fig. 1.

The transport measurements were carried out using the usual four-contacts methods in a conventional He⁴ cryostat and two of the samples (S1,S2) were also measured in a dilution refrigerator. Static magnetic fields were provided by superconducting solenoids applied al-

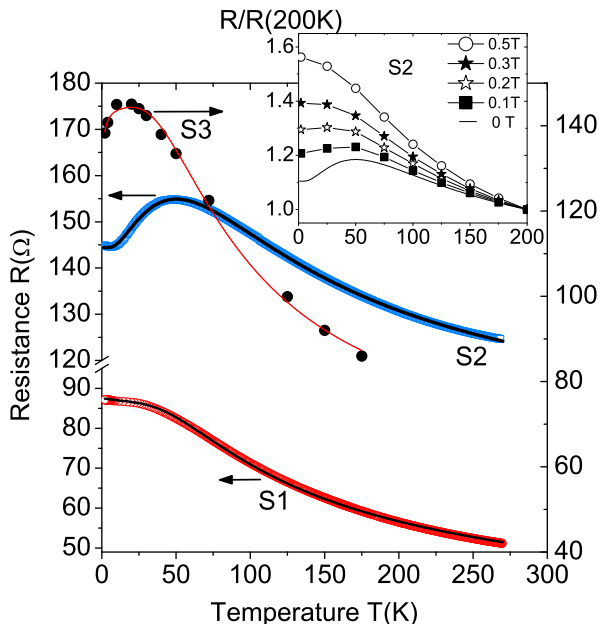


FIG. 2. Resistance vs. temperature for the three multi-graphene samples discussed in this work. The measurements were made without any applied field. The continuous lines were calculated following the parallel-resistor model from Ref. 26, see text. The inset shows the normalized resistance vs. temperature at different fields applied normal to the interfaces for sample S2.

ways parallel to the c -axis. The longitudinal and transverse resistances were measured using a low-frequency AC bridge LR700 (Linear Research). After checking the ohmic response in both voltage electrodes of the samples, all the measurements were done with a fixed current of $1 \mu\text{A}$, which means a dissipation $dQ/dt < 0.1 \text{ nW}$ to avoid self heating effects. In this work we focus on the Hall coefficient obtained at fields $\mu_0 H \lesssim 0.2 \text{ T}$.

III. RESULTS AND DISCUSSION

A. Temperature dependence of the longitudinal resistance

Figure 2 shows the electrical longitudinal resistance of the three samples vs. temperature at zero applied field. Following the results and the discussion exposed in Ref. 26, we assume that ideal graphite is a narrow-gap semiconductor. The observed semiconducting-like temperature dependence in the longitudinal resistance has been also reported recently for thin graphite flakes¹⁹. We assume that any deviation from a semiconducting-like dependence in the longitudinal resistance is due to extrinsic contributions. The observed behavior in our samples is similar to that already published²⁵ and it can

be understood taking into account the contributions of the semiconducting graphene layers in parallel to that from the embedded interfaces and of the sample surfaces (open and with the substrate)²⁶. The interfaces' contribution is responsible for the maximum in the resistance observed at $\sim 50 \text{ K}$ and $\sim 20 \text{ K}$ for samples S2 and S3, respectively. We speculate that the sample surfaces are responsible for the saturation of the resistance at low temperatures, as in S1 for example. The embedded interface contribution appears to be weaker in sample S1 than in the other two samples, therefore we expect for this sample a Hall coefficient with less extrinsic contributions than for the other two.

With a simple parallel-resistor model one can understand quantitatively the measured temperature dependence using different weights between the parallel contributions following the relation²⁶:

$$R(T) = (R_i^{-1}(T) + R_b^{-1}(T))^{-1}, \quad (1)$$

see Fig. 2. The bulk, intrinsic contribution of graphite is semiconducting-like

$$R_b^{-1}(T) \simeq (A \exp(E_g/2k_B T))^{-1} + R_d^{-1}, \quad (2)$$

and the one from the interfaces and surfaces can be simulated following

$$R_i(T) = R_0 + R_1 T + R_2 \exp(-E_a/k_B T), \quad (3)$$

whereas the parameters $A, R_j (j = 0, 1, d)$ are free. The constant term R_d prevents an infinite resistance from the bulk contribution, which is physically related to defects or (a) surface band(s). E_g, E_a denote the semiconducting gap and an activation energy; their values depend on sample within the range $250 \text{ K} \lesssim E_g \lesssim 500 \text{ K}$ and $10 \text{ K} \lesssim E_a \lesssim 50 \text{ K}$ ²⁶. The linear in temperature term ($R_1 T$) could be negative or positive and it is taken as a guess for the contribution of the surfaces and/or metallic-like interfaces. The thermally activated function can be interpreted as the contribution of non-percolative, granular superconducting regions inside the internal interfaces embedded in the graphite matrix²⁶, similar to that observed in granular Al in a Ge matrix⁴², for example. Transport²⁷ as well as magnetization²⁸ measurements support the existence of granular superconductivity and Josephson coupling between superconducting regions at these interfaces.

At fields of the order of 0.1 T applied perpendicular to the interfaces, the metallic-like behavior (at $T < 50 \text{ K}$) starts to vanish, see the results of sample S2 in the inset of Fig. 2, as example. This behavior is assigned to the field-driven superconductor- (or metal-) insulator transition^{20,43-45}. Because this behaviour is absent in thin enough graphite flakes^{25,26} or in thicker graphite samples without well defined interfaces, the field-driven transition is not intrinsic of ideal graphite and should not be interpreted in terms of band models for graphite with Bernal stacking order^{44,45}. If this field-driven transition

is compatible with the existence of Josephson coupled superconducting regions at the interfaces^{26–28}, we therefore expect that the Hall coefficient should be influenced at similar applied fields, as we show below.

B. Temperature dependence of the low-field Hall coefficient

The low-field Hall coefficient is defined as the $R_H^0 = d \lim_{H \rightarrow 0} r_H / \mu_0 H$, where r_H is the Hall resistance and d the measured thickness of the sample. Figure 3 shows the temperature dependence of $R_H^0(T)$ for the three samples measured in this work. We note that it changes sign at ~ 45 K and ~ 70 K for samples S3 and S2. For sample S1, $R_H^0(T)$ remains positive in the whole measured temperature range. The observed behavior of R_H^0 for sample S1 as well as its absolute value are similar to the recently reported ones for a mesoscopic graphite flake of similar thickness¹⁹. Due to the large dispersion of Hall coefficients and their variation with temperature found in literature (see Table I in Sec. I), this agreement is remarkable and support early results on a positive R_H^0 at low enough fields and temperatures for graphite^{1,11}.

All the three samples show positive, saturating $R_H^0(T \lesssim 25$ K), see Fig. 3. The origin of the differences between the low-field Hall coefficients at low temperatures is not known with certainty. A quantitative comparison of the absolute values of the Hall coefficient between different graphite samples is not straightforward because different samples have different interface contributions. The density of these interfaces as well as the number of those that have superconducting properties depend on the sample and it is not simply proportional to the thickness of the sample. Also different absolute values could arise from differences between the properties of holes and electron carriers, see Eq. (4), whose densities and mobilities can be influenced by defects and impurity atoms. Therefore, differences in the absolute values of the Hall coefficient between the samples should be taken with some care.

1. The intrinsic Hall coefficient

Taking into account the T -dependence of the longitudinal resistance, the results of Ref. 26 and the fact that $R_H^0(T)$ is positive, at least a two-band model² is necessary to interpret the data. According to this model, the Hall coefficient is given by:

$$R_H^0 = \frac{\mu_p^2 p - \mu_n^2 n}{e(\mu_p p + \mu_n n)^2}, \quad (4)$$

where $\mu_{p,n}$ are the mobilities for holes with density p and electrons with density n , respectively; e is the positive defined electronic charge. Since $R_H^0 > 0$, then $\mu_p^2 p > \mu_n^2 n$.

Taking into account the expected band structure of graphite and for practical purposes, we can assume either: (1) both mobilities are equal and that the carrier densities are related through $p = n + \delta > n$ with $\delta \ll p, n$, or (2) $\mu_p = \mu_n + \delta > \mu_n$, $p = n$ and $\delta \ll \mu_p, \mu_n$. In both cases $p + n \simeq 2p$ and Eq. (4) can be approximated by either:

$$R_H^0 \simeq \frac{\delta}{4ep^2} \text{ with } \delta = p - n \quad (5)$$

or

$$R_H^0 \simeq \frac{\delta}{2ep\mu_p} \text{ with } \delta = \mu_p - \mu_n. \quad (6)$$

Obviously, the use of the one-band model equation, i.e. $R_H^0 = 1/pe$, provides incorrect values for the carrier concentration. For example, in Ref. 19 the authors obtained $p(77 \text{ K}) \simeq 7.7 \times 10^{19} \text{ cm}^{-3}$ or $p_{2D}(77 \text{ K}) \simeq 2.5 \times 10^{12} \text{ cm}^{-2}$ per graphene layer. Using the same one-band model we would obtain for sample S1, $p_{2D} \simeq 8 \times 10^{12} \text{ cm}^{-2}$, a value four orders of magnitude larger than the one obtained for similar samples using a model independent constriction method⁴⁶. Moreover, for such large p values the use of Eq. (5) would give $\delta \gtrsim p$ using the measured R_H^0 . However, if we take the carrier concentration $p_{2D}(75 \text{ K}) \simeq 5 \times 10^8 \text{ cm}^{-2}$ (or $p_{3D} \simeq 1.6 \times 10^{16} \text{ cm}^{-3}$) from Ref. 46, using Eq. (5) we obtain $\delta/p = 2.5 \times 10^{-4}$, indicating a very small difference between electron and hole carrier densities. Or using Eq. (6) we obtain $\delta/\mu_p \simeq 1 \times 10^{-4}$, indicating a very small difference between the electron and Hall mobilities.

For sample S1, $R_H^0(T)$ can be understood as the parallel contributions⁴⁷ from the graphene layers with $p(T), n(T) \propto \exp(-E_g/2k_B T)$ and a roughly temperature independent term (from the surfaces or some internal interfaces) that prevents the divergence of $R_H^0(T \rightarrow 0)$. Using the same energy gap that fits the longitudinal resistance, we can fit $R_H^0(T)$ in the whole T -range, see Fig. 3.

2. Interface contribution to the Hall coefficient

The results for $R_H^0(T)$ of sample S1 and those from ref. 19 indicate us that the sign change above certain temperature in samples S3 and S2 should be related with the contribution of interfaces. Real graphite samples with interfaces are rather complex systems in the sense that the distribution of input electrical currents inside the sample is not homogeneous. Without knowing this distribution and the intrinsic conductivities of the different contributions, quantitative models are only under certain assumptions applicable. To estimate the interface contribution we use the model proposed in Ref. 47 for a bilayer, where the Hall coefficient of the surface (in our case the interfaces $R_H^i(T)$) and bulk ($R_H^b(T)$) contribute in parallel. The total measured Hall coefficient is given by

$$R_H = \frac{d(R_H^b \sigma_b^2 d_b + R_H^i \sigma_i^2 d_i)}{(\sigma_b d_b + \sigma_i d_i)^2}, \quad (7)$$

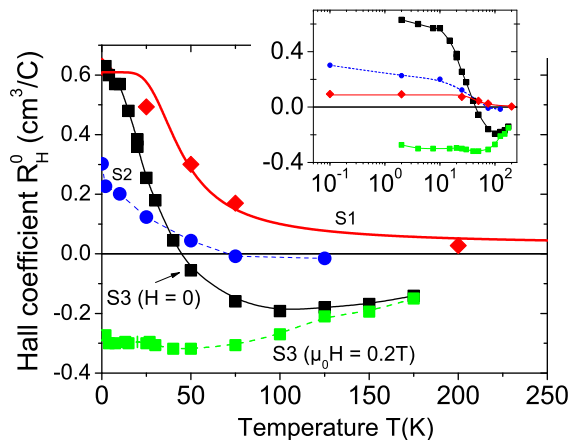


FIG. 3. Temperature dependence of the low-field Hall coefficient for the three studied samples. For sample S3 (black squares) we show also the Hall coefficient (green squares) obtained at a field $\mu_0 H = 0.2$ T applied normal to the interfaces. The data from sample S1 in the main panel of the figure were multiplied by a constant factor of 6.7. The inset shows the same data but in a logarithmic temperature scale. The line through the S1 data points follows the function $R_H^0 = (11^{-1} + (4 \times 10^{-3} \exp(300/(2T)))^{-1})^{-1}$. All other lines are only a guide to the eye.

where $\sigma_{b,i}$ are the conductivities of the bulk and interface contributions and $d_{b,i}$ the respective effective thicknesses, i.e. the total thickness of the sample is $d = d_b + d_i$. Taking into account the interface density in our HOPG samples obtained from transmission electron microscopy²⁵, we estimate $d_i/d_b \lesssim 10^{-2}$. In this case Eq. (7) can be written as:

$$R_H \sim \frac{R_H^b + R_H^i r_2}{r_1}, \quad (8)$$

$$r_1 = (1 + r_1')^2, r_1' = \frac{\sigma_i d_i}{\sigma_b d_b}, \quad (9)$$

$$r_2 = \frac{\sigma_i^2 d_i}{\sigma_b^2 d_b} = r_1'^2 \frac{d_b}{d_i}. \quad (10)$$

The effective parallel contribution of the interfaces can be estimated from

$$R_H^i \sim \frac{R_H r_1 - R_H^b}{r_2}. \quad (11)$$

In clear contrast to sample S1, the $R_H^0(T)$ of sample S3 turns to negative at $T > 45$ K. We propose that the origin for the sign change of $R_H^0(T)$ increasing T is due to the extra contribution of the interfaces when the superconducting properties of the interfaces vanish. At low enough temperatures the interfaces with the superconducting regions²⁷ do not contribute substantially to the total low-field Hall effect. Because we are dealing here with the zero- or low-field Hall coefficient, vortices or fluxons (and their movement) are not expected to influence the Hall signal.

For sample S3 and using Eq. (11) we assume that $R_H^i(T \ll 50 \text{ K}) \simeq 0$ implying $R_H^0 r_1 \gg R_H^b$. If we assume further that the total low-field Hall coefficient for this sample and at low temperatures is mainly given by the bulk contribution, we can roughly estimate the expected contribution from the interfaces. Using the functions that fit the temperature dependence of the measured resistance, see Fig. 2, the related conductivities can be estimated from $\sigma_i^{-1} \sim g_i(140 - 0.045T + 10 \exp(-4/T))$ and similarly for the bulk contribution $\sigma_b^{-1} \sim g_b(80 \exp(350/2T))$, where the constant prefactors $g_{b,i} \sim w_{b,i} \times d_{b,i}/\ell_{b,i}$ (width \times thickness / length) are due to the different effective geometry of the two contributions. Note that neither the samples have perfectly rectangular shape nor the internal interfaces are expected to follow perfectly the measured external sample geometry. We estimate the Hall coefficient due to the bulk contribution as $R_H^b(T) \sim (20^{-1} + (0.1 \exp(350/2T))^{-1})^{-1}$ assuming that the saturation of R_H^0 we measured for this sample, see Fig. 4, can be included in R_H^b . Assuming $d_b/d_i = 50$, we estimate the interface contribution to the Hall coefficient using Eq. (11) for three values of the factor $w_b \ell_i / w_i \ell_b$ that enters in r_1' . The three curves can be seen in Fig. 4. The uncertainty in the geometrical factors and in the bulk Hall contribution do not allow a better quantitative estimate of the interface contribution. Nevertheless, qualitatively the obtained results for $R_H^i(T)$ appear reasonable.

C. Magnetic field dependence of the Hall coefficient

We emphasize that for graphite samples with no measurable evidence for the interface contribution, in the electrical resistivity for example, the Hall coefficient does not depend on the field, at least up to 1 T applied normal to the graphene planes^{18,19}. Therefore, a direct way to test our assumption that the Hall coefficient and its negative value is not intrinsic – but due to the extra contribution from the embedded interfaces with superconducting regions – can be independently done measuring it at finite magnetic fields applied normal to the interfaces. In this case we expect that a magnetic field will have the same influence on the interface contribution as the temperature. In other words, a large enough magnetic field will destroy the coupling between the superconducting regions, or the superconductivity itself at the interfaces and an extra, electron-like contribution should be measurable, in principle in the whole temperature range. Note that mostly electron-like carriers are expected to be at the interfaces with a density of the order of $\lesssim 10^{12} \text{ cm}^{-2}$. This is inferred from Shubnikov-de Haas (SdH) oscillations in the magnetoresistance obtained in samples with and without (or with less number of) interfaces, see, e.g., Ref. 25 (compare there samples L5 and L7) or Ref. 48 where a clear decrease in the amplitude of the SdH oscillations decreasing the thickness of the samples has been reported

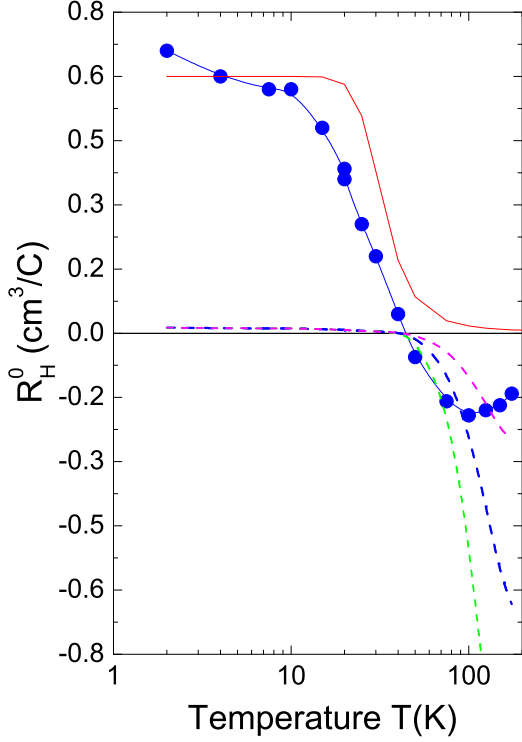


FIG. 4. Temperature dependence of the low-field Hall coefficient for the S3 sample. The red line follows the equation $R_H^b = 0.03(20^{-1} + (0.1 \exp(350/(2T)))^{-1})^{-1}$ used as the bulk contribution to the Hall coefficient for that sample. The dashed lines represent the contribution from the interfaces $R_H^i(T)$ calculated from Eq. (11) assuming different geometrical ratios $w_b \ell_i / w_i \ell_b = 200, 300, 500$, from bottom to top lines, respectively.

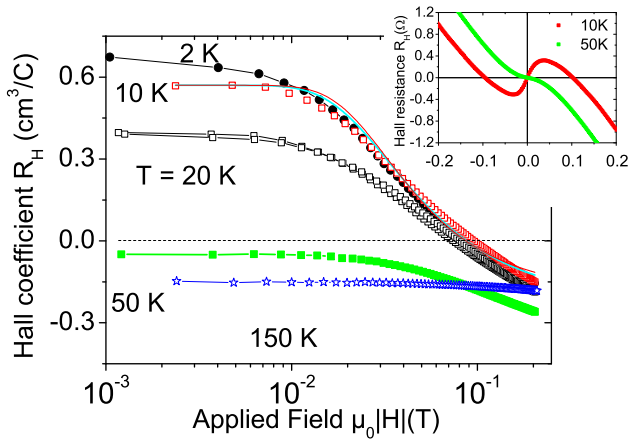


FIG. 5. Hall coefficient as a function of the absolute value of the applied field at several temperatures for sample S3. The inset shows the field dependence of the Hall resistance at two temperatures.

earlier. The reason why mostly electron-like carriers appear to be at the interfaces is related to the nature of the interfaces themselves, a subject that is being discussed nowadays, see Ref. 29 and Refs. therein. For example, in addition to the twist angle between the graphite Bernal blocks forming an interface, one has extra doping through hydrogen or carbon vacancies that influence the carrier density and the superconducting regions at the interfaces. For interfaces without superconducting regions we expect an electron-like contribution to the Hall coefficient with a weaker field and temperature dependence.

How large should be the magnetic field to affect the coupling between the superconducting regions or the superconductivity of the regions itself? An estimate of this field can be directly obtained from the longitudinal resistance and the metal-insulator transition (MIT) observed in several high grade graphite samples, as, e.g., in sample S2, see inset in Fig. 2, or several other samples reported in literature^{20,44,45,49}. From all the results for the longitudinal resistance we expect that a field of the order of 0.1 T should be sufficient to influence substantially the Hall coefficient contribution of the interfaces. Note that the MIT of graphite is absent for samples without or with negligible amount of interfaces^{18,19,25,26}. Figure 3 shows the Hall coefficient of sample S3 at a field of 0.2 T. It remains nearly temperature independent below 100 K and matches the results obtained at low-fields at high enough temperatures.

Figure 5 shows the field dependence of R_H at various constant temperatures where we recognize a transition from positive to negative values at fields similar to those necessary to trigger the metal-insulator transition observed in the longitudinal resistance. The results shown in this figure clearly indicate that a magnetic field has the same influence on the Hall coefficient as temperature. Note also that a field of the order of 0.1 T is enough to change the sign of the Hall coefficient in the sample with clear contribution of the interfaces.

Apart from the interface effects, one may expect a decrease of the (positive) Hall coefficient with field, at large enough fields when the cyclotron energy $\hbar\omega_c$ is of the order of the energy gap E_g ($\omega_c = e\mu_0 H/m^*$ and m^* the effective electron mass, according to Ref. 50). Because in graphite $E_g \lesssim 50$ meV this effect may start be observable at $\mu_0 H > 1$ T. On the other hand, data obtained from very thin graphite samples clearly show that the Hall coefficient is field independent up to 10 T at $T = 0.1$ K¹⁸, or up to 1 T at $T \geq 77$ K¹⁹. Therefore, we can clearly argue that the observed field dependence in our sample, see Fig. 5, is not intrinsic of the graphite structure but has an extrinsic origin, similar to that reported earlier^{1,11}.

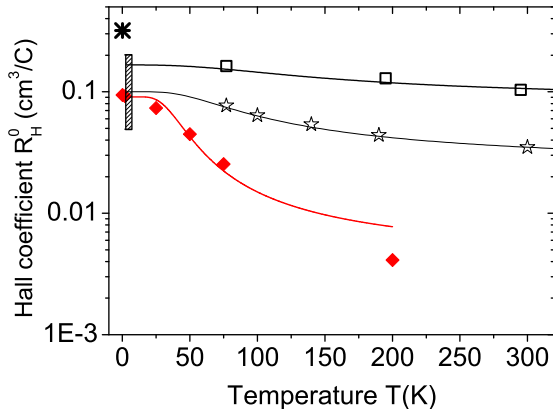


FIG. 6. Low-field Hall coefficient as a function of temperature for sample S1 from this work (red lozenges); the line through the points follows the equation $(11 + (0.004 \exp(300/2T))^{-1})^{-1}$. The other points are taken from different graphite samples reported in literature. (\star): Taken from Ref. 19 for a graphite thin flake; the line through the points follows the equation $(10 + (0.03 \exp(350/2T))^{-1})^{-1}$. (\square): Taken from Ref. 12; the line through the points follows the equation $(6 + (0.15 \exp(400/2T))^{-1})^{-1}$. The vertical dashed region at low temperatures with $0.05 \leq R_H^0 \leq 0.2 \text{ cm}^3/\text{C}$ is from Ref. 14. (\star): Hall coefficient at 100 mK obtained for a 5 nm thick graphite sample from Ref. 18.

IV. COMPARISON WITH LITERATURE AND CONCLUSION

In a recent theoretical work⁵¹, the magnetoresistance and Hall resistivity for graphite has been calculated using the usual 3D band structure described by the Slonczewski-Weiss-McClure model and taking into account only some of its six free parameters⁵². The obtained results indicate that at relatively weak applied magnetic fields $< 1 \text{ T}$, the magnetoresistance increases linearly with field due to the presence of extremely light, Dirac-like carriers. Interestingly, in the same field range the authors found that the Hall coefficient should be positive and proportional to $\ln|B|$. We note that a linear field magnetoresistance was indeed reported in this field range and at low T in a large amount of graphite samples, especially for relatively thick graphite samples, see for example the magnetoresistance curves for sample L7 (75 nm thick) in Ref. 25. Due to the observed positive Hall effect at low fields $< 0.2 \text{ T}$ and at low temperatures, it is of interest to check whether such a linear field dependence is observed in the samples described in this work. Figure 7 shows the magnetoresistance vs. applied field below 0.2 T for the three samples and at low temperatures. Interestingly, none of the samples show a clear linear field dependence. The sample S1, which has the smallest contribution from interfaces (see Fig. 2) follows approximately a $H^{1.5}$ dependence. The other two sam-

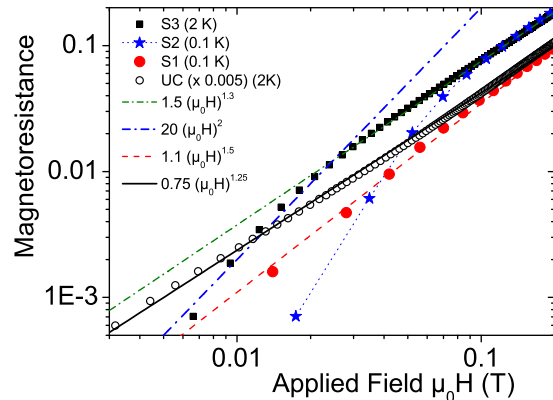


FIG. 7. Low-field magnetoresistance defined as $R(B) - R(0)/R(0)$ vs. applied field in a double logarithmic scale, for the three samples studied in this work. The data of samples S1 and S2 were taken at 0.1 K and of sample S3 at 2 K. In the same panel we show the data for a bulk HOPG sample of grade A (\circ) obtained at 2 K.

ples, S2 and S3 tends to follow a quadratic dependence at low enough fields changing to a $\sim H^{1.3}$ dependence at higher fields, in agreement with similar measurements but in bulk HOPG samples⁵³. Note that the absolute value of the magnetoresistance at a given field for our mesoscopic samples is much smaller than in bulk samples. As an example, we show in Fig. 7 the results for a bulk HOPG sample of grade A. In the depicted field region the magnetoresistance follows $\sim H^{1.25}$ but it is 200 times larger than in the other mesoscopic samples. This difference might be related to the size dependence of the magnetoresistance when the mean free path is of the order of the sample size^{46,54}. The field dependence in this low field region, however, does not seem to be affected.

We note that in the same field range we did not see an increasing Hall coefficient with field in any of the samples studied here. Also, for the graphite samples reported in Ref. 19 at $T \geq 77 \text{ K}$ the Hall coefficient is constant below 1 T and decreases above. In the case of the $\simeq 1 \times 1 \mu\text{m}^2$ sample reported in Ref. 18 we note that the magnetoresistance is negligible to 10 T applied field and $T = 0.1 \text{ K}$, a result related to the ballistic behavior of the carriers due to their large mean free path⁴⁶, and the Hall coefficient does not depend on field.

A comparison of the Hall coefficient and in general of the Hall data from literature is not straightforward because the sample quality as well as the existence of interfaces (of any kind) was not provided in any of the publications and remains, in general, unknown. Nevertheless, we can speculate the following trends and provide a possible answer to the works listed in Tab. I. In Refs. 12 and 13, a positive Hall effect was observed for small grains only. Upon preparation conditions, smaller grains should have less interfaces, see section I, and therefore less contribu-

tion from them. Note that the reported dependence of R_H on the *alignment* of the crystallites can be directly related to the larger probability to have well-defined and larger interfaces the larger the alignment of the crystallites is. Note that effective critical temperature depends on the size or area of the interfaces according to recently published experimental results⁴¹. The crossover to a negative Hall coefficient at large enough fields and temperatures observed in Refs. 1, 8, 14, and 15 can be understood in a similar way as shown in sections III B 2 and III C. In Ref. 11 the Hall coefficient was reported to be positive for samples with long mean free path of the carriers and negative for samples with smaller mean free path or high fields. The crossover to a negative R_H can be understood in the same way if some of the interfaces get normal conducting with field. Now, the reported mean free path dependence of R_H cannot be simply interpreted in terms of interfaces contribution without knowing the internal structure of the samples and whether there is or not a crossover to negative R_H at higher fields and temperatures. If we assume that the carriers in the graphene layers of graphite have much larger mobility⁴⁶ than those carriers at the interfaces in the normal state, we may speculate that samples with smaller mean free path have larger density of interfaces and therefore a negative R_H should be measured.

The negative QHE measured in the HOPG samples in Refs. 20 and 21 at high fields should come from normal conducting interfaces with a relatively high density of carriers. Note that those HOPG samples are the ones that show a high density and well-defined two-dimensional interfaces²⁵. That the QHE is not observed in all HOPG samples, even when they are from the same grade⁸ (or even batch) is related to a non-homogeneous distribution of the interfaces. The observation of the AHE in Ref. 22 is related to defects that trigger magnetic order⁵⁵. Note that even in a mesoscopic graphite

sample one can find different contributions to the transport depending how homogeneous the sample is, see e.g., Ref. 56. Therefore, in this kind of samples it is difficult to measure the intrinsic contribution coming from the ideal graphene layers. Finally, the positive R_H measured in Refs. 18 and 19 can be expected since those samples were very probably free from interfaces due to their small thickness.

In general we can state that at low enough fields and in thin enough samples with low density of interfaces, the Hall coefficient should be closer the one from the ideal bulk graphite than at higher fields. Therefore we show in Fig. 6 low-field coefficients obtained from old and recent publications at different temperatures, in case these data were available. From all these data, we conclude that the intrinsic, low magnetic field Hall coefficient of graphite appear to be positive with a low-temperature value around $0.1 \text{ cm}^3/\text{C}$ and a temperature dependence that follows closely that of a semiconductor with an energy gap of the order of 400 K, in agreement with the fits of the longitudinal resistance of different samples²⁶. Note that the results shown in Fig. 6 were obtained from graphite samples with very different shapes, i.e. bulk samples in Refs. 12 and 14 and mesoscopic samples with different areas in Refs. 18 and 19. From this comparison we would conclude that the low temperature value of the Hall coefficient does not seem to strongly depend on the defined Hall geometry.

In conclusion, taking into account the contribution of superconducting regions at certain interfaces found in real graphite samples, we provide a possible explanation for the anomalous temperature and low magnetic field behavior of the Hall coefficient as well as for its differences between samples of different origins reported in the last 60 years.

We thank Yakov Kopelevich for fruitful discussion. Part of this work has been supported by EuroMagNET II under the EC contract 228043.

* esquin@physik.uni-leipzig.de

¹ D. E. Soule, Phys. Rev. **112**, 698 (1958).

² B. T. Kelly, *Physics of Graphite* (London: Applied Science Publishers, 1981).

³ A. Grüneis, C. Attacalite, T. Pichler, V. Zabolotnyy, H. Shiozawa, S. L. Molodtsov, D. Inosov, A. Koitzsch, M. Knupfer, J. Schiessling, R. Follath, R. Weber, P. Rudolf, R. Wirtz, and A. Rubio, Phys. Rev. Lett. **100**, 037601 (2008).

⁴ S. Y. Zhou, G.-H. Gweon, J. Graf, A. V. Fedorov, C. D. Spataru, R. Diehl, Y. Kopelevich, D.-H. Lee, S. G. Louie, and A. Lanzara, Nature Physics **2**, 595 (2006).

⁵ S. Y. Zhou, G.-H. Gweon, and A. Lanzara, Annals of Physics **321**, 1730 (2006).

⁶ C. S. Leem, B. J. Kim, C. Kim, S. R. Park, T. Ohta, A. Bostwick, E. Rotenberg, H. D. Kim, M. K. Kim, H. J. Choi, and C. Kim, Phys. Rev. Lett. **100**, 016802 (2008).

⁷ K. Sugawara, T. Sato, S. Souma, T. Takahashi, and

H. Suematsu, Phys. Rev. Lett. **98**, 036801 (2007).

⁸ J. M. Schneider, M. Orlita, M. Potemski, and D. K. Maude, Phys. Rev. Lett. **102**, 166403 (2009), see also the comment by I. A. Luk'yanchuk and Y. Kopelevich, idem **104**, 119701 (2010).

⁹ M. Orlita, C. Faugeras, G. Martinez, D. K. Maude, M. L. Sadowski, J. M. Schneider, and M. Potemski, Journal of Physics: Condensed Matter **20**, 454223 (2008).

¹⁰ N. A. Goncharuk, L. Nádvořník, C. Faugeras, M. Orlita, and L. Smrčka, Phys. Rev. B **86**, 155409 (2012).

¹¹ J. D. Cooper, J. Woore, and D. A. Young, Nature **721–722**, 225 (1970).

¹² G. H. Kinchin, Proc. R. Soc. Lond. A **217**, 1128 (1953).

¹³ S. Mrozowski and A. Chaberski, Phys. Rev. **104**, 74 (1956).

¹⁴ N. B. Brandt, G. A. Kapustin, V. G. Karavaev, A. S. Kotosonov, and E. A. Svistova, Sov. Phys.-JETP **40**, 564 (1974).

¹⁵ H. Oshima, K. Kawamura, T. Tsuzuku, and K. Sugihara,

- J Phys. Soc. Japan **51**, 1476 (1982).
- ¹⁶ J. C. Slonczewski and P. R. Weiss, Physical Review **109**, 272 (1958).
 - ¹⁷ J. W. McClure, Physical Review **112**, 715 (1958).
 - ¹⁸ J. S. Bunch, Y. Yaish, M. Brink, K. Bolotin, and P. L. McEuen, Nano Letters **5**, 287 (2005).
 - ¹⁹ R. Vansweevelt, V. Mortet, J. DHaen, B. Ruttens, C. V. Haesendonck, B. Partoens, F. M. Peeters, and P. Wagner, Phys. Status Solidi A **208**, 1252 (2011).
 - ²⁰ Y. Kopelevich, J. H. S. Torres, R. R. da Silva, F. Mrowka, H. Kempa, and P. Esquinazi, Phys. Rev. Lett. **90**, 156402 (2003).
 - ²¹ H. Kempa, P. Esquinazi, and Y. Kopelevich, Solid State Communications **138**, 118 (2006).
 - ²² Y. Kopelevich, J. M. Pantoja, R. da Silva, F. Mrowka, and P. Esquinazi, Phys. Lett. A **355**, 233 (2006).
 - ²³ Y. Kopelevich and P. Esquinazi, Adv. Mater. (Weinheim, Ger.) **19**, 4559 (2007).
 - ²⁴ M. Inagaki, *New Carbons: Control of Structure and Functions* (Elsevier, 2000) Chap. 2.
 - ²⁵ J. Barzola-Quiquia, J.-L. Yao, P. Rödiger, K. Schindler, and P. Esquinazi, phys. stat. sol. (a) **205**, 2924 (2008).
 - ²⁶ N. García, P. Esquinazi, J. Barzola-Quiquia, and S. Dusari, New Journal of Physics **14**, 053015 (2012).
 - ²⁷ A. Ballestar, J. Barzola-Quiquia, T. Scheike, and P. Esquinazi, New J. Phys. **15**, 023024 (2013).
 - ²⁸ T. Scheike, P. Esquinazi, A. Setzer, and W. Böhlmann, Carbon **59**, 140 (2013).
 - ²⁹ P. Esquinazi, T. T. Heikkilä, Y. V. Lysogoskiy, D. A. Tayurskii, and G. E. Volovik, JETP Letters **100**, 336 (2014), arXiv:1407.1060.
 - ³⁰ J. H. Warner, M. H. Römmeli, T. Gemming, B. Büchner, and G. A. D. Briggs, Nano Letters **9**, 102 (2009).
 - ³¹ L. Feng, X. Lin, L. Meng, J.-C. Nie, J. Ni, , and L. He, Appl. Phys. Lett. , 113113 (2012).
 - ³² P. San-Jose and E. Prada, Phys. Rev. B **88**, 121408(R) (2013).
 - ³³ G. E. Volovik, Proceedings of Nobel Symposium 156: "New forms of Matter - Topological Insulators and Superconductors" (2014), arXiv:1409.3944.
 - ³⁴ N. B. Kopnin, T. T. Heikkilä, and G. E. Volovik, Phys. Rev. B **83**, 220503 (2011).
 - ³⁵ N. B. Kopnin, M. Ijäs, A. Harju, and T. T. Heikkilä, Phys. Rev. B **87**, 140503 (2013).
 - ³⁶ G. E. Volovik, J Supercond Nov Magn **26**, 2887 (2013).
 - ³⁷ W. A. Muñoz, L. Covaci, and F. Peeters, Phys. Rev. B **87**, 134509 (2013).
 - ³⁸ N. B. Kopnin and T. T. Heikkilä, "Surface superconductivity in rhombohedral graphite," ArXiv:1210.7075.
 - ³⁹ Q. Lin, T. Li, Z. Liu, Y. Song, L. He, Z. Hu, Q. Guo, and H. Ye, Carbon **50**, 2369 (2012).
 - ⁴⁰ S. Hattendorf, A. Georgi, M. Liebmann, and M. Morgenstern, Surface Science **610**, 53 (2013).
 - ⁴¹ A. Ballestar, T. T. Heikkilä, and P. Esquinazi, Superc. Sci. Technol. **27**, 115014 (2014).
 - ⁴² Y. Shapira and G. Deutscher, Phys. Rev. B **27**, 4463 (1983).
 - ⁴³ H. Kempa, Y. Kopelevich, F. Mrowka, A. Setzer, J. H. S. Torres, R. Höhne, and P. Esquinazi, Solid State Commun. **115**, 539 (2000).
 - ⁴⁴ T. Tokumoto, E. Jobiliong, E. Choi, Y. Oshima, and J. Brooks, Solid State Commun. **129**, 599 (2004).
 - ⁴⁵ X. Du, S.-W. Tsai, D. L. Maslov, and A. F. Hebard, Phys. Rev. Lett. **94**, 166601 (2005).
 - ⁴⁶ S. Dusari, J. Barzola-Quiquia, P. Esquinazi, and N. García, Phys. Rev. B **83**, 125402 (2011).
 - ⁴⁷ R. L. Petritz, Phys. Rev. **110**, 1254 (1958).
 - ⁴⁸ Y. Ohashi, K. Yamamoto, and T. Kubo, Carbon'01, An International Conference on Carbon, Lexington, KY, United States, July 14-19, Publisher: The American Carbon Society, available at www.acs.omnibooksonline.com , 568 (2001).
 - ⁴⁹ Y. Kopelevich, P. Esquinazi, J. H. S. Torres, R. R. da Silva, and H. Kempa, "Graphite as a highly correlated electron liquid," (B. Kramer (Ed.), Springer-Verlag Berlin, 2003) pp. 207–222.
 - ⁵⁰ M. H. Cohen and L. M. Falicov, Phys. Rev. Lett. **7**, 231 (1961).
 - ⁵¹ H. K. Pal and D. L. Maslov, Phys. Rev. B **88**, 035403 (2013).
 - ⁵² N. B. Brandt, S. M. Chudinov, and Y. G. Ponomarev, *Semimetals: I. Graphite and its Compounds* (North-Holland, Amsterdam, 1988).
 - ⁵³ Y. Kopelevich, J. C. M. Pantoja, R. R. da Silva, and S. Moehlecke, Phys. Rev. B **73**, 165128 (2006).
 - ⁵⁴ J. C. González, M. Muñoz, N. García, J. Barzola-Quiquia, D. Spoddig, K. Schindler, and P. Esquinazi, Phys. Rev. Lett. **99**, 216601 (2007).
 - ⁵⁵ P. Esquinazi, W. Hergert, D. Spemann, A. Setzer, and A. Ernst, Magnetics, IEEE Transactions on **49**, 4668 (2013).
 - ⁵⁶ J. Barzola-Quiquia and P. Esquinazi, J Supercond Nov Magn **23**, 451 (2010).